International Journal of Biological Macromolecules 242 (2023) 125056

Contents lists available at ScienceDirect

International Journal of Biological Macromolecules

journal homepage: www.elsevier.com/locate/ijbiomac

Debranching facilitates malate esterification of waxy maize starch and decreases the digestibility

Yizhe Yan [a,c,*], Hong An [a], Yanqi Liu [a], Xiaolong Ji [a], Miaomiao Shi [a], Bin Niu [b,*]

[a] College of Food and Bioengineering, Henan Key Laboratory of Cold Chain Food Quality and Safety Control, Food Laboratory of Zhongyuan, Zhengzhou University of Light Industry, Zhengzhou 450000, PR China
[b] College of Food Science and Technology, Henan Agricultural University, Zhengzhou 450000, PR China
[c] Key Laboratory of Cold Chain Food Processing and Safety Control (Zhengzhou University of Light Industry), Ministry of Education, PR China

ARTICLE INFO

Keywords:
Waxy maize starch
Malate esterification
Debranching
Degree of substitution
Resistant starch

ABSTRACT

In this study, the debranching followed by malate esterification was employed to prepare malate debranched waxy maize starch (MA-DBS) with a high degree of substitution (DS) and low digestibility using malate waxy maize starch (MA-WMS) as the control. The optimal esterification conditions were obtained using an orthogonal experiment. Under this condition, the DS of MA-DBS (0.866) was much higher than that of MA-WMS (0.523). A new absorption peak was generated at 1757 cm^{-1} in the infrared spectra, indicating the occurrence of malate esterification. Compared with MA-WMS, MA-DBS had more particle aggregation, resulting in an increase in the average particle size from scanning electron microscopy and particle size analysis. The X-ray diffraction results showed that the relative crystallinity decreased after malate esterification, in which the crystalline structure of MA-DBS almost disappeared, which was consistent with the decrease of decomposition temperature by thermogravimetric analysis and the disappearance of the endothermic peak by differential scanning calorimeter. *In vitro* digestibility tests showed an order: WMS > DBS > MA-WMS > MA-DBS. The MA-DBS showed the highest content of resistant starch (RS) of 95.77 % and the lowest estimated glycemic index of 42.27. In a word, pullulanase debranching could produce more short amylose, promoting malate esterification and improving the DS. The presence of more malate groups inhibited the formation of starch crystals, increased particle aggregation, and enhanced resistance to enzymolysis. The present study provides a novel protocol for producing modified starch with higher RS content, which has potential application in functional foods with a low glycemic index.

1. Introduction

Starch, as the primary energy source in life, exists in a large number of staple foods. The content of rapidly digestible starch (RDS) in most native starch is high, while the content of slowly digestible starch (SDS) and resistant starch (RS) are low. Therefore, long-term use of starch-based foods can lead to the outbreak of many chronic diseases [1]. Recently, native starches have been modified to decrease their digestibility through different methods, including physical modification, chemical modification, and enzymatic modification [2,3]. Enzymatic and physical modification can rearrange starch molecules, and chemical modification can significantly change the chemical structure of starch [4]. In addition to the common single modification, dual modification has also been applied to the modification of starch [5], such as microwave/heat-moisture treatment [6], hydroxypropylation/cross-linking [7], branching enzyme/transglucosidase [8], citric acid esterification/heat-moisture treatment [9].

Debranching is a process of enzymatic treatment of starch molecules using pullulanase or isoamylase, in which the α-1,6 glycosidic bonds of amylopectin are broken and the branched structure is cut off to generate shorter linear molecules [10]. Thus, new properties and functionality of debranched starch (DBS) are formed. Due to its good hydrogel properties, DBS has been widely used in drug controlled-release [11]. The rapid formation of a gel network structure also reflects its good barrier properties and can be used for coatings [12]. In addition, DBS has good mobility and facilitates molecular assembly, increasing SDS or RS content [13].

As an important method of chemical modification, the esterification of hydroxyl groups in starch under certain conditions has been used to obtain various esterified starch, which is mainly divided into inorganic

* Corresponding authors.
E-mail addresses: yanyizhe@zzuli.edu.cn (Y. Yan), niubin@henau.edu.cn (B. Niu).

https://doi.org/10.1016/j.ijbiomac.2023.125056
Received 2 September 2022; Received in revised form 15 April 2023; Accepted 21 May 2023
Available online 26 May 2023

acid starch esters (such as starch phosphate, starch sulfate, *etc.*) and organic acid starch esters (acetate starch, citrate starch, octenyl succinate starch, *etc.*). The esterification can decrease the digestibility and improve the RS content of starch because substituent groups in esterified starch (RS4) can inhibit the attack of enzymes [14,15]. At present, esterified starch has been used in emulsifier and encapsulating agents [16], drug delivery [17], and wastewater treatment [18].

Malic acid (MA) is one of the food additives and occurs naturally in fruits. MA is oxidized to obtain oxaloacetic acid, which is an important intermediate product of internal circulation and metabolism in the human body. Our previous study has shown that malate esterification increased the content of RS in various botanical starches, but their degree of substitution (DS) was relatively low [19]. Overall, with the increase of the degree of substitution, the digestibility decreased and the RS content increased. Debranching before esterification can provide more reaction sites for esterification, thus improving the degree of substitution. Therefore, the main aim of this study is to prove that the debranching can promote malate esterification of WMS and reveal the influence mechanism of debranching on malate esterification. This study will provide new insights into improving the DS and RS content of malate starch.

2. Materials and methods

2.1. Materials

Waxy maize starch was purchased from Henan Hengrui Starch Technology Co., Ltd. (Luohe, China). Malic acid was purchased from Fuchen Chemical Reagent Factory (Tianjin, China). Three specific enzymes, pullulanase (1000 NPUN/g, E.C.3.2.1.41), pancreatin (8 × USP, P7545), and amyloglucosidase (260 U/mL, A7095), were obtained from Sigma-Aldrich Trading Co., Ltd. (Shanghai, China). A glucose oxidase-peroxidase (GOPOD) assay kit was acquired from Megazyme International Ireland Ltd. (Wicklow, Ireland). All other chemicals are of analytical grade.

2.2. Methods

2.2.1. Preparation of DBS

WMS (5 g, dry weight, $M_w = 2.20 \times 10^7$ g/mol) was prepared into a 10 % (m/w) solution. Then the solution was heated in a water bath for 30 min and then sterilized at 121 °C for 20 min. After cooling to 50 °C, pullulanase (200 μL) was added, and the debranching treatment was carried out by shaking in a water bath (SHZ-82, Jiangsu, China) at 50 °C for 24 h. After the debranching, the sample was heated in a boiling water bath for 30 min to inactivate the enzyme. Absolute ethanol was added into the solution to precipitate (1:2). The solution samples were centrifuged at 4000 rpm by a centrifuge (LG10–24, Beijing, China,), and washed many times with ethanol to obtain solid samples, which were further freeze-dried in a freeze-dryer (Scientz-10 N, Ningbo, China) for 48 h, and screened (100 mesh) to obtain DBS ($M_w = 1.24 \times 10^5$ g/mol).

2.2.2. Malate esterification of DBS and WMS

Malate esterification of DBS was performed using our previous method with minor modifications [18]. The DBS (5 g, dry weight) was made into a solution of 20 % (m/v), and then MA was added at a certain ratio of MA to starch (0.5, 0.6, or 0.7, *w*/w). The pH value of the mixture was adjusted to 1.5, 2.0, or 2.5 with NaOH (10 mol/L, 1 mol/L, and 0.5 mol/L) solution, placed at room temperature for 11 h, and then dried at 50 °C until the water content was <10 %. After crushing, it was placed in a glass dish and reacted for 6 h at a certain temperature (130, 140, or 150 °C). The crude product was washed many times to remove excess MA until pH was neutral. The malate-esterified DBS (MA-DBS) was obtained by drying at 45 °C, grinding and sifting (100 mesh). Malate-esterified waxy maize starch (MA-WMS) was obtained as a control according to the above method.

2.2.3. Determination of DS

DS of malate starch was determined using our previous method with minor modifications [19]. The malate starch (0.5 g, dry weight) was added to 50 mL of water, and 2–3 drops of phenolphthalein solution were dropped. After dropping NaOH solution (0.1 mol/L) until the color of the solution changed to red, 5 mL of NaOH solution (0.5 mol/L) was added and stirred for 20 min. The mixture was titrated with HCl standard solution (0.5 mol/L) to neutralize excess NaOH. Meanwhile, WMS was taken as a blank.

The mass fraction of MA substituents (A) was calculated from the following Eq. (1):

$$A\% = \left(\frac{V_2}{M_2} - \frac{V_1}{M_1}\right) \times C \times 117 \times 100 \quad (1)$$

DS of malate starch was calculated from the following Eq. (2):

$$DS = \frac{162A}{100 \times 117 - (117 - 1)A} = \frac{162A}{11700 - 116A} \quad (2)$$

In which, A (%) represent the mass fraction of MA substituents; V_1 (L) and V_2 (L) represent the volume of HCl solution consumed by the blank and sample, respectively; C (mol/L) represents the concentration of HCl standard solution used in titration; M_1 (g) and M_2 (g) represent blank and sample mass, respectively; 117 (g/mol) represents the molar mass of 2-hydroxysuccinyl group; 162 (g/mol) represents the molar mass of glucosyl.

2.2.4. Scanning electron microscopy (SEM)

The morphology of WMS, DBS, MA-WMS, and MA-DBS was studied by a high-resolution field emission scanning electron microscope (Regulus 8100, Hitachi, Tokyo, Japan). The dried samples were attached to the sample stage with conductive adhesive and sprayed with gold in the ion sputtering device. The morphology of each sample was photographed with a magnification of 1000 times under an accelerating voltage of 3.0 kV.

2.2.5. Particle size analysis

The particle size distribution of the sample was measured using a Beckman LS13320/ULM2 laser particle size analyzer (UK). The sample was prepared into a 1 % (*w*/w) suspension, add the suspension of 1 mL to the sample tank [20]. Volume D (4,3), D10, D50, and D90 were recorded and analyzed.

2.2.6. X-ray diffraction (XRD)

All starch samples were balanced with saturated NaCl solution for one week before testing [21] and determined by a Bruker D8 Advance X-ray diffractometer (Karlsruhe, Germany). The test conditions are as follows: voltage 30 kV, current 20 mA, scanning speed 4°/min, scanning range 5°-35°, scanning step 0.02°. The relative crystallinity (RC) of starch is the percentage of the crystalline region of starch granules in the total starch granules, which is used to characterize the crystalline properties of starch granules. The RC of the sample was calculated by the following Eq. (3) [22]:

$$RC(\%) = \frac{A_c}{A_c + A_a} \quad (3)$$

where A_c is the area of the crystalline region, and A_a is the area of the amorphous region.

2.2.7. Fourier transform infrared spectroscopy (FTIR)

The corresponding FTIR spectra of starch samples were measured by a FTIR spectrometer (Vertex 70, Bruker, Karlsruhe, Germany). 3 mg (dry weight) of sample and 0.3 g of KBr were dried at 45 °C and 105 °C for 4–5 h, respectively, mixed and pressed. The resolution of 4 cm^{-1} and the scanning time of 64 s were taken as the conditions to obtain the spectrum of 4000–400 cm^{-1}. The FTIR spectra were analyzed by using

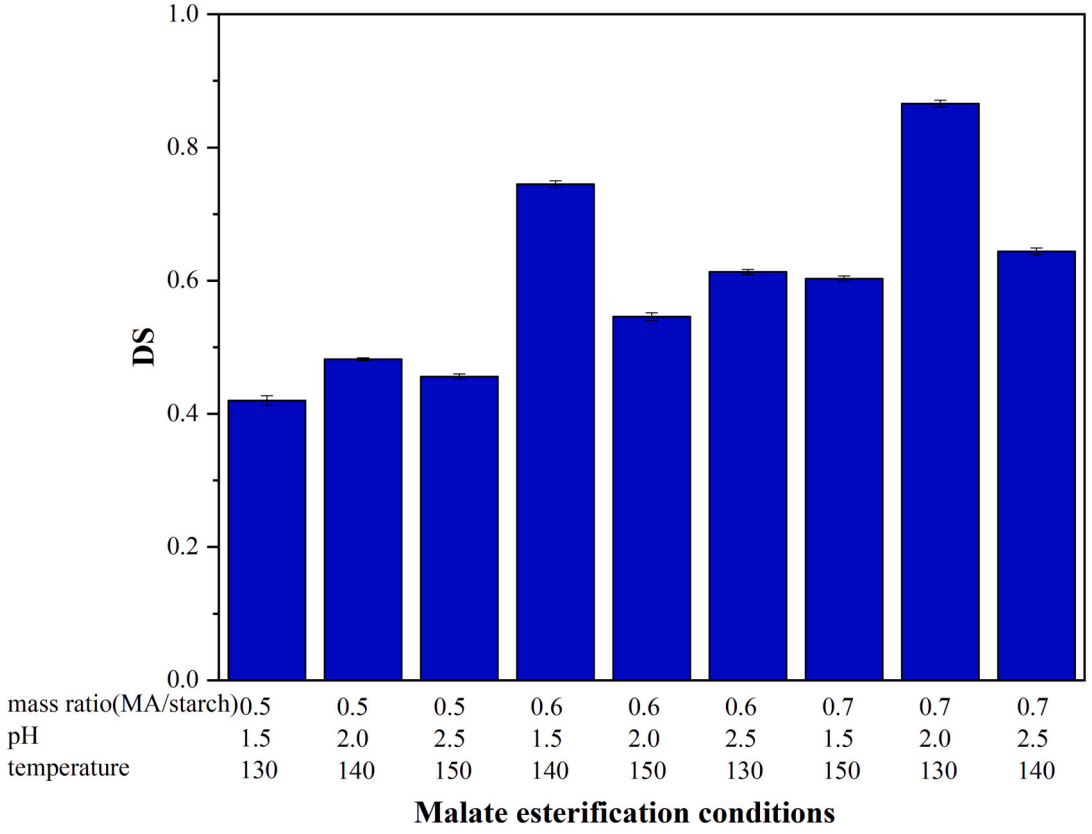

Fig. 1. The DS of MA-DBS under various conditions in orthogonal experiment.

OMNIC software, and the baseline was corrected automatically.

2.2.8. Thermogravimetric analysis (TGA)

Thermogravimetric analysis of starch samples was conducted by a synchronous thermal analyzer (Diamond TG/DTA, Norwalk, America). The starch samples (3 mg) were placed in a ceramic dish, sealed, and heated from 30 °C to 600 °C at a heating rate of 10 °C/min under nitrogen [23].

2.2.9. Differential scanning calorimetry (DSC)

The thermal properties of starch samples were determined by a differential scanning calorimeter (Q20, TA Instruments, Newcastle, DE, USA). The starch sample (3 mg, dry basis) and distilled water were added to the aluminum pan for a 12 mg of total weight. The aluminum pan was sealed, placed at room temperature for 24 h to balance moisture, and then heated from 10 °C to 120 °C at 10 °C/min using an empty aluminum pan as a reference simultaneously. The thermal properties of starch were analyzed by TA2000 analysis software.

2.2.10. In vitro digestibility

In vitro digestibility of starch was determined by our previous method with some modifications [24]. 2 g of pancreatin was dissolved in 14 mL of distilled water, stirred for 10 min, and centrifuged at 3000 rpm for 20 min to obtain the supernatant. Then amyloglucosidase (0.53 mL) and distilled water (1.17 mL) were added into the supernatant, and mixed well to form the amylase mixture. Sodium acetate buffer (4 mL, 0.1 mol/L) was added to the test tube containing 200 mg (dry weight) of the starch sample. Then the starch sample was gelatinized completely by heating at 100 °C for 30 min in a constant temperature water bath pot. After cooling to 37 °C, the amylase mixture (1 mL) was added for hydrolysis at 37 °C and 200 rpm for 6 h. At different times (20, 40, 60, 90, 120, 180, 240, and 360 min), the same amount of hydrolysate (0.1 mL) was added to the test tube containing 4 mL of 70 % ethanol for inactivation. After centrifugation at 3000 rpm, 0.1 mL of the supernatant was used to measure the content of hydrolyzed glucose at 510 nm by GOPOD. Similarly, 0.1 mL of blank solution, standard solution (1.0 mg/mL standard glucose solution) and water were measured using the same method to obtain the blank absorbance, standard absorbance, and water absorbance, respectively. The contents of RDS, SDS, and RS were calculated from the following Eqs. (4)–(7) [25]:

$$C\ (\%) = \frac{A_t - A_0}{A_1 - A_2} \times \frac{5.2 \times 4}{0.1 \times 200} \times 100 \times 0.9 \tag{4}$$

$$\mathrm{RDS}(\%) = (G_{20} - FG) \times 0.9 \tag{5}$$

$$\mathrm{SDS}(\%) = (G_{120} - G_{20}) \times 0.9 \tag{6}$$

$$\mathrm{RS}(\%) = 1 - \mathrm{RDS} - \mathrm{SDS} \tag{7}$$

In which, C represents the hydrolysis percentage of starch at 20–360 min; A_t, A_0, A_1 and A_2 represent the absorbance of samples, blank absorbance, standard absorbance, and water absorbance at 20–360 min, respectively; G_{20} and G_{120} represent the glucose content after hydrolysis for 20 and 120 min, respectively; FG represents the glucose content of the sample before hydrolysis.

The hydrolysis curve of starch was fitted according to the Eq. (8) [26]:

$$C = C_\infty \left(1 - e^{-kt}\right) \tag{8}$$

The curve area (AUC) in the range of 0–180 min was calculated, and the estimated glycemic index (eGI) was predicted by the Eq. (9) [26]:

$$eGI = 39.71 + 0.549\ HI \tag{9}$$

In the above equation, k represents the hydrolysis rate constant; C represents the hydrolysis percentage at t time; C_∞ represents the equilibrium concentration; HI represents the ratio of AUC (sample) to AUC

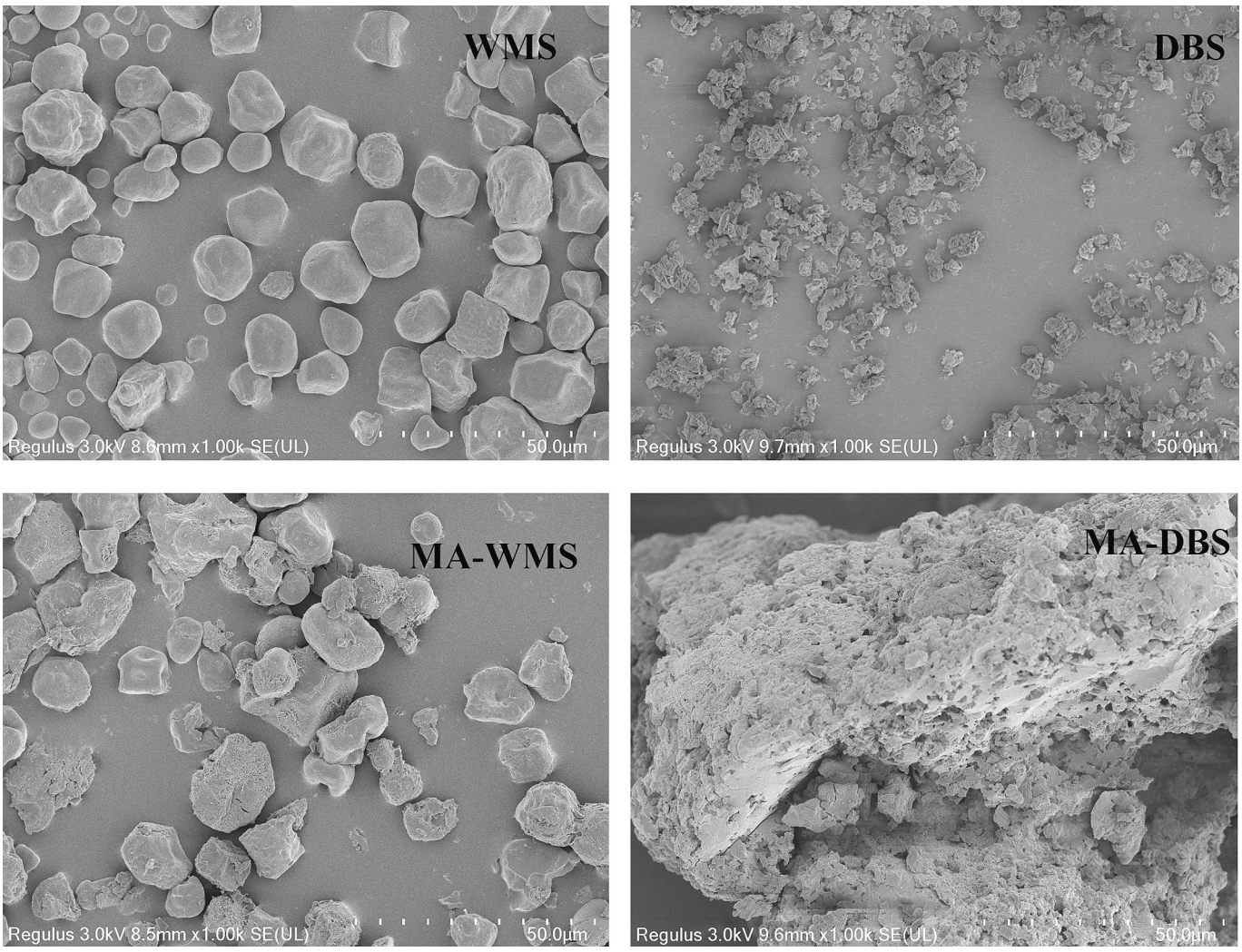

Fig. 2. SEM images of WMS, DBS, MA-WMS, and MA-DBS.

(white bread).

2.2.11. Statistical analysis

All the experiments were repeated in triplicate, and experimental results were composed of the means value and standard deviation. The analysis of variance tool in IBM SPSS Statistics 26 (Chicago, IL, USA) was used to analyze the data. The analysis of variance (ANOVA) by Duncan's test was performed to compare the means ($p < 0.05$).

3. Results and discussion

3.1. Establishment of optimal conditions

According to prior single-factor experiments, the L_9 (3^4) orthogonal table is used to carry out the orthogonal test using DS as the experimental index, and mass ratio of MA to starch, pH value, and temperature as the experimental factors. The orthogonal experimental results were shown in Fig. 1. After range analysis, the optimal esterification conditions were obtained. When the mass ratio was 0.7, the pH value was 2, and the temperature was 130 °C, the highest DS of 0.866 was obtained. Moreover, the sequence of the factors was determined according to the results of range analysis: mass ratio > temperature > pH value. Increasing the amount of MA could increase the DS of malate starch, which was similar to citrate esterification [27]. Relatively high temperature (130 °C) could stimulate molecular motion and increase the contact chance of starch molecules with MA, thereby increasing the DS. However, excessive high temperature (150 °C) may decompose the starch, thereby reducing the DS. Lower pH favors the formation of malic anhydride, but too low pH could result in acidolysis of starch and starch esters. Under the same conditions, WMS was esterified to obtain MA-WMS with a DS of 0.523. Compared with native starch, pullulanase broke the α-1,6 glycosidic bonds in amylopectin and generated more hydroxyl groups to react with malic anhydride [28]. It can be concluded that the debranching process could significantly facilitate malate esterification and improve the DS of malate starch.

3.2. Particle morphology

The differences in particle morphology of WMS, DBS, MA-WMS, and MA-DBS prepared under optimal esterification conditions, were presented in Fig. 2. The surface of WMS particles was relatively smooth, complete in shape, polyhedral, or oval. After debranching, DBS granules became small, irregular and piled up with each other. After malate esterification, MA-WMS had passive edges and a rough surface, while the integrity of whole starch particles still retained. The large area aggregation and loose structure of MA-DBS particles might be due to the appearance of a large number of hydroxyl groups after debranching, which could provide more reaction sites for esterification. The more combination of MA and starch could promote the adhesion and aggregation of starch particles.

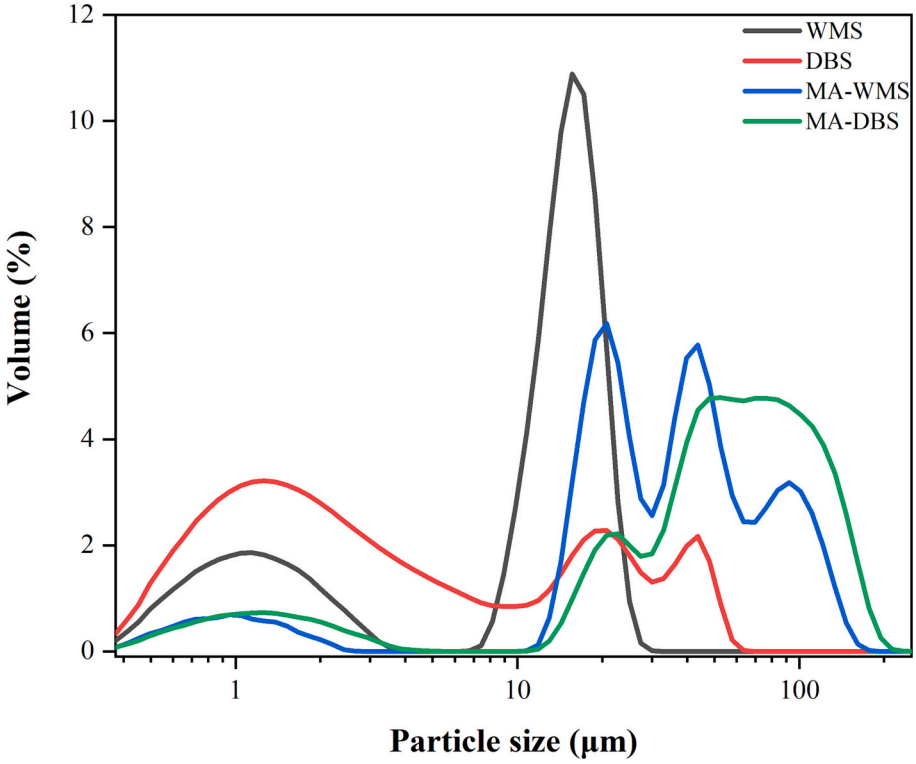

Fig. 3. Particle size distribution of WMS, DBS, MA-WMS, and MA-DBS.

Table 1
Particle size of WMS, DBS, MA-WMS, and MA-DBS.

Samples	D (4,3) (μm)	D10 (μm)	D50 (μm)	D90 (μm)
WMS	12.116 ± 0.060^{c}	0.948 ± 0.001^{c}	14.022 ± 0.009^{c}	20.613 ± 0.002^{d}
DBS	9.158 ± 0.006^{d}	0.751 ± 0.010^{d}	2.594 ± 0.013^{d}	31.845 ± 0.001^{c}
MA-WMS	39.249 ± 0.364^{b}	16.553 ± 0.591^{b}	42.564 ± 0.043^{b}	86.699 ± 0.586^{b}
MA-DBS	73.208 ± 3.672^{a}	19.133 ± 0.439^{a}	74.207 ± 2.862^{a}	155.520 ± 3.289^{a}

Values are expressed as means ± SD of three measurements. Means with different lowercase letters in the same column indicate significant differences ($p < 0.05$).
D (4.3) is the volume average diameter. D10, D50, and D90 are the particle sizes at 10, 50, and 90 % of the volume of all particles, respectively.

3.3. Particle size distribution

There were obvious changes in the particle size distribution of the four samples from Fig. 3. The order of the average particle size was DBS < WMS < MA-WMS < MA-DBS (Table 1). After debranching, the particle size of DBS was obviously reduced, and a large number of smaller particles was formed (D50 = 2.594 ± 0.013 μm) due to the generation of a large number of short amylose, which was consistent with the results of SEM. The size of starch granules after malate esterification was significantly larger than that of the original starch. In the process of esterification, the crystal structure of starch was destroyed, and the surface was eroded, which led to an increase in starch roughness and improved the adhesion of starch [29]. This resulted in the aggregation of starch granules and the formation of larger particle sizes. In addition, the particle size of MA-DBS was significantly larger than that of MA-WMS. This may be due to the enhanced esterification of short starch molecules, which leads to the aggregation of more starch molecules.

3.4. Crystalline structure

The differences in the X-ray diffraction patterns of four starch samples were presented in Fig. 4. WMS displayed prominent diffraction peaks at 15.1°, 17.1°, 18.0°, and 23.0°, which was a typical A-type crystal form. In addition to the characteristic peaks of A-type starch, DBS also displayed diffraction peaks at 7.8°, 13.4°, and 20.3°, which were the characteristic peaks of V-type crystal form, indicating the formation of single helical structure of starch. Therefore, DBS was a mixture of A-type and V-type crystal forms, similar to Miao's study [30]. The RC of DBS (22.87 %) was lower than that of WMS (31.40 %), which proved that the crystalline structure of starch was damaged to a certain extent during the debranching process because pullulanase broke the α-1,6 glycosidic bonds in amylopectin and inhibited the double helix structure of amylopectin. The intensity of diffraction peaks and RC of MA-WMS was significantly reduced compared with native starch due to esterification. Notably, weaker diffraction peaks were observed in the XRD pattern of MA-DBS, which was because the increased reaction of DBS with malic anhydride destroyed the crystalline structure [31].

3.5. FTIR spectra

The changes in functional groups of starch molecules were distinguished by FTIR. The infrared spectra of WMS, DBS, MA-WMS, and MA-DBS were shown in Fig. 5. Compared with WMS, the intensity of absorption peak at 3404 cm^{-1} of DBS increased, which was due to the production of more hydroxyl groups by the debranching of WMS. However, the hydroxyl characteristic peak of MA-WMS and MA-DBS shifted towards the higher wave number of 3466 cm^{-1} because the malate esterification destroyed the hydrogen bonds of hydroxyl groups in starch molecules. Meanwhile, the peak intensity of malate starch was weaker than that of native and debranched starch because the number of free hydroxyl groups was decreased *via* the esterification of hydroxyl with MA [29]. In addition, the peak intensity of MA-DBS was weaker than that of MA-WMS at 3466 cm^{-1}, indicating enhanced esterification.

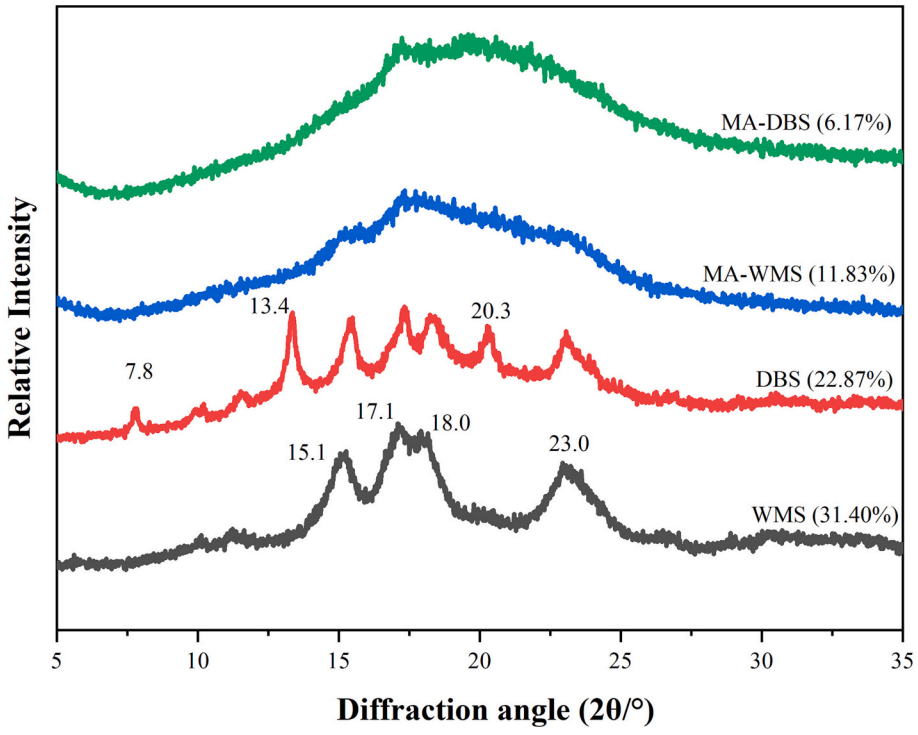

Fig. 4. X-ray diffraction patterns and crystallinity of WMS, DBS, MA-WMS, and MA-DBS. The brackets are expressed as relative crystallinity.

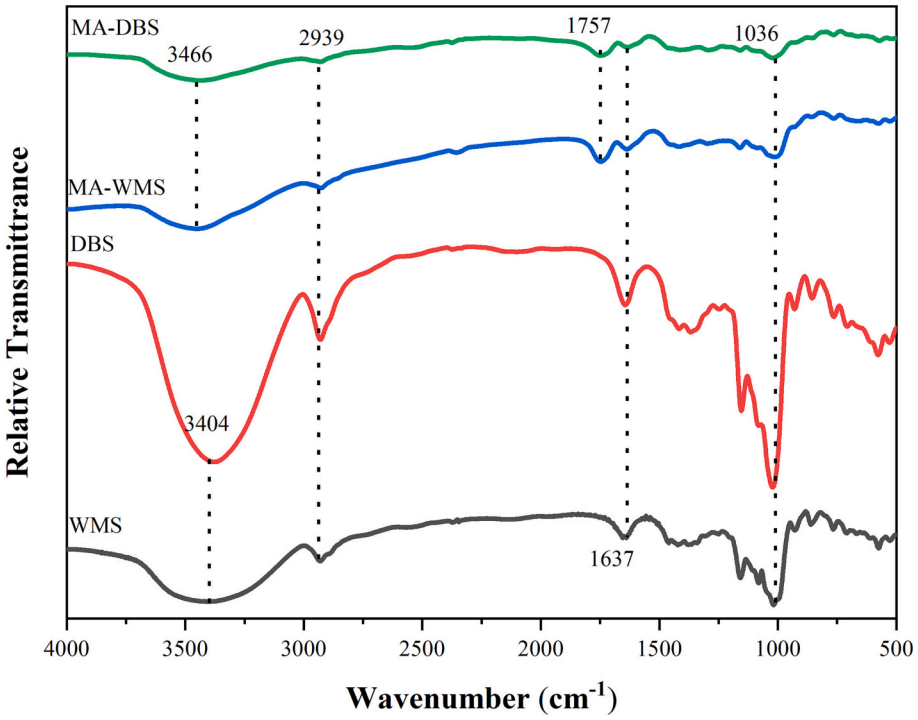

Fig. 5. FTIR spectra of WMS, DBS, MA-WMS, and MA-DBS.

Notably, a new characteristic peak appeared at 1757 cm^{-1} in the infrared spectra of MA-WMS and MA-DBS, which was closely related to the formation of ester bonds by malate esterification [32]. The weakening of the peak intensity at 1637 cm^{-1} also proved the occurrence of esterification reaction [33].

3.6. Thermal properties

Through thermogravimetric analysis, the thermal stability and thermal loss rate of starch were understood. As shown in Fig. 6A, all starch samples had two weightlessness intervals. The first interval basically started at about 80 °C, and the loss in this stage mainly came from the evaporation of free water in the starch samples. The second

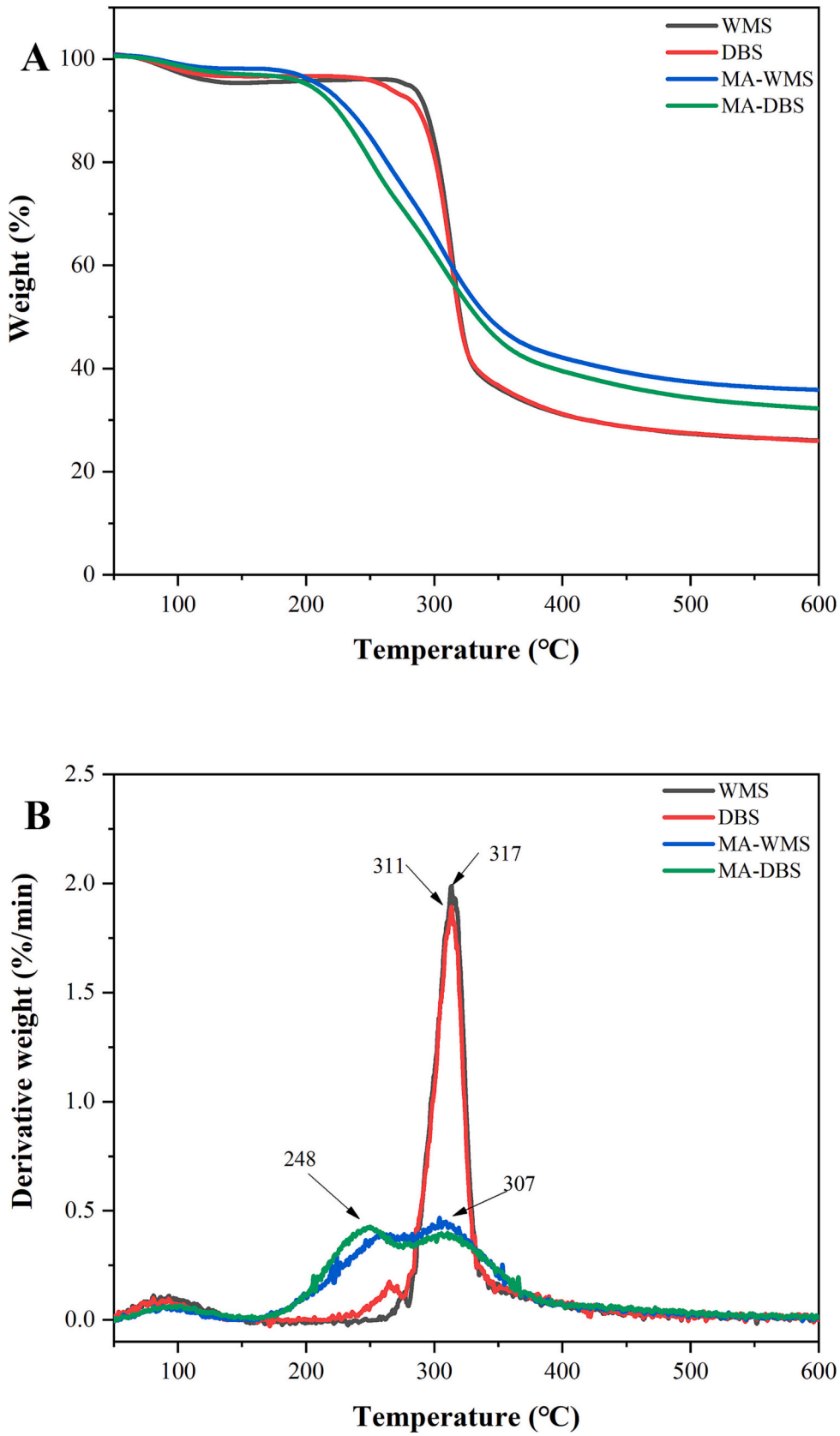

Fig. 6. TGA curves of WMS, DBS, MA-WMS, and MA-DBS.

Table 2
Thermal and gelatinization properties of WMS, DBS, MA-WMS, and MA-DBS.

Samples	WMS	DBS	MA-WMS	MA-DBS
Weightlessness Interval (°C)	289.45–345.81	272.01–343.02	165.75–372.35	166.16–377.63
Maximum weightlessness temperature (°C)	317.21 ± 1.47^{a}	310.63 ± 0.64^{b}	307.07 ± 0.71^{c}	248.26 ± 1.19^{d}
T_o (°C)	63.83 ± 0.47^{b}	69.51 ± 0.81^{a}	N.D.	N.D.
T_p (°C)	70.58 ± 0.34^{b}	94.31 ± 0.65^{a}	N.D.	N.D.
T_c (°C)	80.53 ± 0.40^{b}	113.94 ± 0.40^{a}	N.D.	N.D.
ΔH (J/g)	14.03 ± 0.23^{a}	11.52 ± 0.43^{b}	N.D.	N.D.

Values are expressed as means ± standard deviation of three measurements. Means with different lowercase letters in the same line indicate significant differences ($p < 0.05$).
T_o—onset temperature; T_p—peak temperature; T_c—conclusion temperature; ΔH—gelatinization enthalpy.

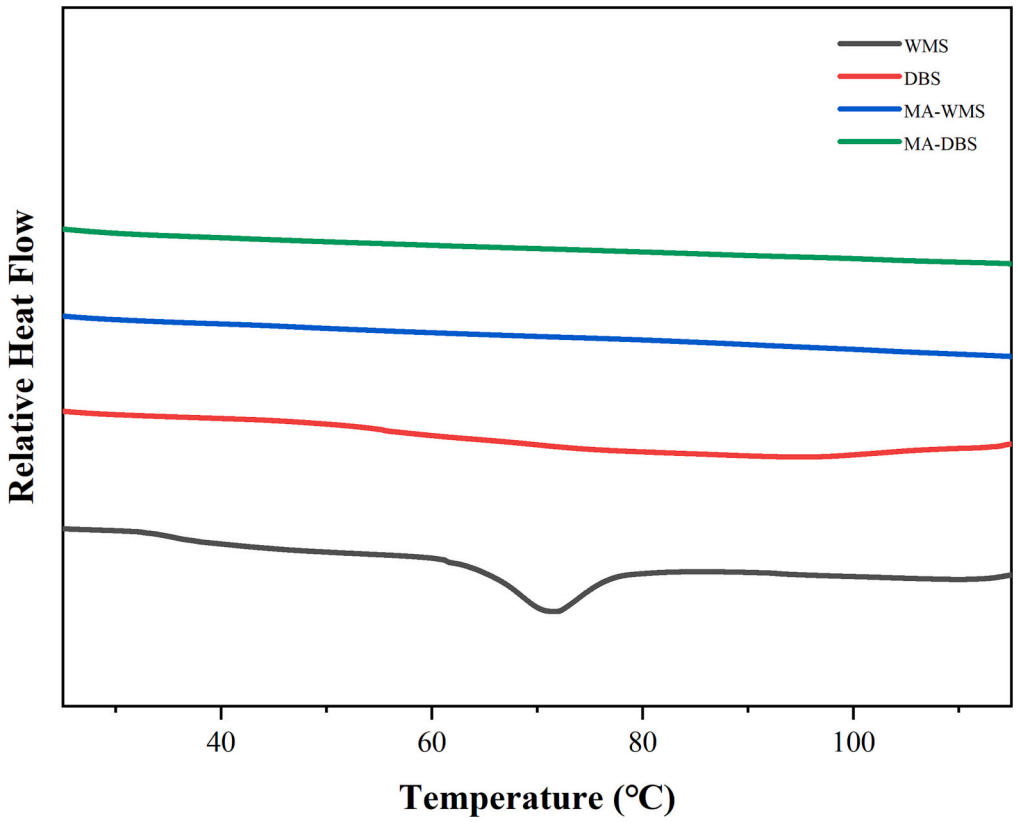

Fig. 7. DSC curves of WMS, DBS, MA-WMS, and MA-DBS.

weightlessness interval was caused by the decomposition of starch molecules under the action of high temperature, which was consistent with the description of Abral [34]. The changes in decomposition temperature of starch samples were shown in Table 2. The weight loss ranges of WMS and DBS were 289.45–345.81 °C and 272.01–343.02 °C, and the maximum weightlessness temperatures were 317.21 °C and 310.63 °C, respectively. In contrast, the weight loss ranges of MA-WMS and MA-DBS were 165.75–372.35 °C and 166.16–377.63 °C, and the maximum weightlessness temperatures were 307.07 °C and 248.26 °C, respectively. After esterification, the weightlessness range of malate starch became relatively more extensive, and the maximum weightlessness temperature became lower. When the crystallinity decreases, the chemical bond that needs to be destroyed for cracking decreases, so the maximum weight loss temperature decreases [31,35]. Therefore, according to the results of XRD and previous studies, compared with MA-WMS, the maximum weight loss temperature of MA-DBS decreases further due to the increase of amorphous region.

3.7. Gelatinization properties

According to the DSC curves of the four starch samples (Fig. 7), the onset temperature (T_o), peak temperature (T_p), conclusion temperature (T_c), and gelatinization enthalpy (ΔH) were all summarized in Table 2. Compared with WMS, the endothermic range and gelatinization temperature (T_o, T_p, T_c) of DBS increased while ΔH decreased due to the formation of V-type crystals and the decrease of the helix structure [36]. It was worth noting that the endothermic peak of malate starch disappeared due to the destruction of the crystalline structure by malate esterification, which was also consistent with XRD results [37].

3.8. In vitro digestibility

The digestion curve of each sample was displayed in Fig. 8, in which the order of *in vitro* digestibility was WMS > DBS > MA-WMS > MA-DBS. As shown in Table 3, the content of RS in starch was changed from 10.19 % to 19.78 % after the debranching of WMS, which might be because the debranching produced more short linear chains and formed smaller gel structures, thereby inhibiting the digestibility of starch [38].

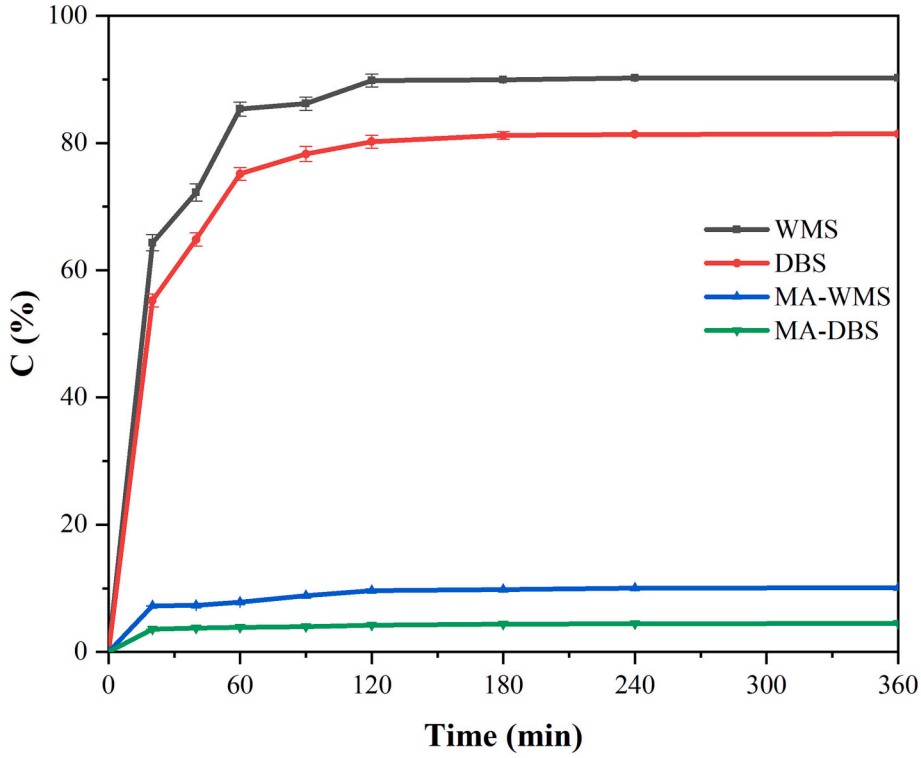

Fig. 8. *In vitro* digestion curves of WMS, DBS, MA-WMS, and MA-DBS.

Table 3
RDS, SDS and RS contents of WMS, DBS, MA-WMS, and MA-DBS.

Samples	RDS (%)	SDS (%)	RS (%)	C_∞ (%)	k (min^{-1})	AUC	eGI
WMS	64.33 ± 1.27^a	25.48 ± 1.29^a	10.19 ± 0.01^d	88.36 ± 0.46^a	0.056 ± 0.003^b	$14{,}241.05 \pm 54.94^a$	92.82 ± 0.21^a
DBS	55.24 ± 0.01^b	24.98 ± 0.03^b	19.78 ± 0.02^c	79.74 ± 0.63^b	0.051 ± 0.001^b	$12{,}722.36 \pm 62.85^b$	87.15 ± 0.23^b
MA-WMS	7.24 ± 0.02^c	2.40 ± 0.28^c	90.36 ± 0.27^b	9.26 ± 0.14^c	0.056 ± 0.003^b	1479.84 ± 18.48^c	45.23 ± 0.07^c
MA-DBS	3.56 ± 0.02^d	0.66 ± 0.00^d	95.77 ± 0.23^a	4.14 ± 0.09^d	0.089 ± 0.011^a	686.66 ± 6.54^d	42.27 ± 0.02^d

Values are expressed as means ± standard deviation of three measurements. Means with different lowercase letters in the same column indicate significant differences ($p < 0.05$). RDS—rapidly digestible starch; SDS—slowly digestible starch; RS—resistant starch C_∞—equilibrium concentration; k—hydrolysis rate constant; AUC—curve area in the range of 0–180 min; eGI—estimated glycemic index.

Compared with WMS and DBS, the content of RS in MA-WMS and MA-DBS was increased to 90.36 % and 95.77 %, respectively [19,31,36]. This was because the steric hindrance of malate substituent in malate starch might inhibit the attack of enzymes, leading to an increase in the content of RS [39]. Moreover, the previous study has shown that starch aggregation was negatively correlated with digestibility, which meant that the higher the degree of aggregation, the lower the digestibility [40]. Thus, more molecular aggregation in malate starch was an important reason for the increase of RS content. Notably, the digestibility of MA-DBS was lower than that of MA-WMS due to the increase of the DS.

eGI represents the response of blood sugar in the body, which is positively correlated with the digestibility of starch. After fitting and calculation, the eGI of four starch samples was obtained. From Table 3, WMS (92.82) and DBS (87.15) belonged to high GI foods, while MA-WMS (45.23) and MA-DBS (42.27) belonged to low GI foods [41]. Among them, the eGI of MA-DBS was the lowest, which could be used in the production of low GI food.

3.9. Correlation analysis

The correlation analysis between multi-scale structure and properties of four starch samples was presented in Table 4. RS content was negatively correlated with RDS content, SDS content, C_∞, eGI, RC, starting weight loss temperature, ΔH, T_o, and T_P, while RS content was positively correlated with D10. The correlation analysis results indicated that *in vitro* digestibility of the starch samples was closely correlated with crystalline structure, particle size, thermal properties, and gelatinization properties. The real reason might be that the pullulanase debranching could produce shorter amylose and promote malate esterification, which resulted in the introduction of more malate groups, inhibited the formation of starch crystals, increased particle aggregation, decreased thermal stability, and enhanced resistance to enzymolysis [42,43].

4. Conclusion

In summary, the pullulanase debranching followed by malate esterification was first used to increase the DS and lower the digestibility of starch. After optimizing the malate esterification conditions, MA-DBS with a DS of 0.866 was prepared using MA-WMS as a control. The new peak at 1757 cm^{-1} in infrared spectra confirmed the success of the esterification reaction. During the process of malate esterification, the intermolecular double helix structure was destroyed, resulting in a decrease of relative crystallinity, more amorphous regions, and lower decomposition temperature. Compared with MA-WMS, MA-DBS had the higher DS and content of RS with more amorphous regions and molecular aggregation. This study provides new insights into improving the

Table 4
Pearson correlation analysis between the structure and properties of WMS, DBS, MA-WMS, and MA-DBS.

	RDS	SDS	RS	C_∞	eGI	D (4,3)	D10	D50	D90	RC	Initial weight loss temperature	Maximum weightlessness temperature	ΔH	T_o	T_p	T_c
RDS	1															
SDS	0.995**	1														
RS	−0.998**	−0.997**	1													
C_∞	0.999**	0.998**	−0.999**	1												
eGI	0.998**	0.997**	−0.999**	1.000**	1											
D (4,3)	−0.904	−0.916	0.092	−0.909	−0.907	1										
D10	−0.990**	−0.998**	0.994**	−0.994**	−0.994**	0.937	1									
D50	−0.903	−0.926	0.911	−0.912	−0.910	0.993**	0.947	1								
D90	−0.915	−0.915	0.916	−0.915	−0.915	0.993**	0.934	0.973*	1							
RC	0.967*	0.943	−0.961*	0.959*	0.960*	−0.909	−0.943	−0.878	−0.943	1						
Initial weight loss temperature	0.999**	0.994**	−0.998**	0.998**	0.999**	−0.884	−0.987*	−0.887	−0.894	0.956*	1					
Maximum weightlessness temperature	0.695	0.694	−0.695	0.694	0.693	−0.916	−0.731	−0.875	−0.925	0.788	0.658	1				
ΔH	0.999**	−0.991**	−0.997**	0.997**	−0.814	−0.881	0.851	−0.880	−0.894	0.962*	1.000**	0.660	1			
T_o	0.983*	0.996**	−0.988*	0.989*	0.998**	−0.896	−0.993**	−0.917	−0.886	0.908	0.986*	0.649	0.980*	1		
T_p	0.949	0.976*	−0.958*	0.960*	0.958*	−0.885	−0.976*	−0.921	−0.859	0.848	0.953*	0.625	0.943	0.990**	1	
T_c	0.936	0.967*	−0.947	0.949	0.947	−0.880	−0.968*	−0.919	−0.849	0.830	0.941	0.616	0.930	0.984*	0.999**	1

** Significant correlation at level 0.01.
* Significant correlation at level 0.05.

DS of esterified starch and lowering its digestibility by debranching pretreatment.

CRediT authorship contribution statement

Yizhe Yan: Conceptualization, Funding acquisition, Supervision, Writing – review & editing. **Hong An:** Formal analysis, Methodology, Writing – original draft. **Yanqi Liu:** Formal analysis, Funding acquisition. **Xiaolong Ji:** Data curation, Formal analysis. **Miaomiao Shi:** Formal analysis. **Bin Niu:** Funding acquisition, Writing – review & editing.

Declaration of competing interest

The authors declare that they have no known competing financial interests or personal relationships that could have appeared to influence the work reported in this paper.

Acknowledgements

This study is supported by the National Natural Science Foundation of China (32101945), the Natural Science Foundation of Henan Province (222300420580), and the Science and Technology Basic Research Program of Henan Province (202102110302). We also acknowledge Shanghai Sanshu Biotechnology Co., LTD for their help in the determination of relative molecular weight of starch.

References

[1] T. Church, C.K. Martin, The obesity epidemic: a consequence of reduced energy expenditure and the uncoupling of energy intake, Obesity 26 (2018) 14–16, https://doi.org/10.1002/oby.22072.
[2] P.B. Sneh, A.O. Ashogbon, A. Singh, V. Chaudhary, W.S. Whiteside, Enzymatic modification of starch: a green approach for starch applications, Carbohydr. Polym. 287 (2022), https://doi.org/10.1016/j.carbpol.2022.119265. Article 119265.
[3] H.X. Xiong Zia-ud-Din, P. Fei, Physical and chemical modification of starches: a review, Crit. Rev. Food Sci. Nutr. 57 (2017) 2691–2705, https://doi.org/10.1080/10408398.2015.1087379.
[4] J.H. Chen, Y.X. Wang, J. Liu, X.L. Xu, Preparation, characterization, physicochemical property and potential application of porous starch: a review, Int. J. Biol. Macromol. 148 (2020) 1169–1181, https://doi.org/10.1016/j.ijbiomac.2020.02.055.
[5] A.O. Ashogbon, Dual modification of various starches: Synthesis, properties and applications, Food Chem. 342 (2021), https://doi.org/10.1016/j.foodchem.2020.128325. Article 128325.
[6] D. Deka, N. Sit, Dual modification of taro starch by microwave and other heat moisture treatments, Int. J. Biol. Macromol. 92 (2016) 416–422, https://doi.org/10.1016/j.ijbiomac.2016.07.040.
[7] B.J. Hazarika, N. Sit, Effect of dual modification with hydroxypropylation and cross-linking on physicochemical properties of taro starch, Carbohydr. Polym. 140 (2016) 269–278, https://doi.org/10.1016/j.carbpol.2015.12.055.
[8] L. Guo, Y.F. Deng, L. Lu, F. Zou, B. Cui, Synergistic effects of branching enzyme and transglucosidase on the modification of potato starch granules, Int. J. Biol. Macromol. 130 (2019) 499–507, https://doi.org/10.1016/j.ijbiomac.2019.02.160.
[9] M.N. Li, Y. Xie, H.Q. Chen, B. Zhang, Effects of heat-moisture treatment after citric acid esterification on structural properties and digestibility of wheat starch, A- and B-type starch granules, Food Chem. 272 (2019) 523–529, https://doi.org/10.1016/j.foodchem.2018.08.079.
[10] G.D. Liu, Z.B. Gu, Y. Hong, L. Cheng, C.M. Li, Structure, functionality and applications of debranched starch: a review, Trends Food Sci. Tech. 63 (2017) 70–79, https://doi.org/10.1016/j.tifs.2017.03.004.
[11] G.D. Liu, Y. Hong, Z.B. Gu, Z.F. Li, L. Cheng, C.M. Li, Preparation and characterization of pullulanase debranched starches and their properties for drug controlled-release, RSC Adv. 5 (2015) 97066–97075, https://doi.org/10.1039/C5RA18701J.
[12] G.D. Liu, Y. Hong, Z.B. Gu, Z.F. Li, L. Cheng, Pullulanase hydrolysis behaviors and hydrogel properties of debranched starches from different sources, Food Hydrocoll. 45 (2015) 351–360, https://doi.org/10.1016/j.foodhyd.2014.12.006.
[13] W. Liu, Y. Hong, Z.B. Gu, L. Cheng, Z.F. Li, C.M. Li, In structure and *in-vitro* digestibility of waxy corn starch debranched by pullulanase, Food Hydrocoll. 67 (2017) 104–110, https://doi.org/10.1016/j.foodhyd.2016.12.036.
[14] H.X. Wei, B.D. Liang, K.Y. Wei, L.P. Xue, S.D. Zeng, X.M. Yin, Effects of high-pressure cooking processing on the physicochemical properties, structure and digestibility of citric acid-esterified starches, Int. J. Food. Sci. Tech. 57 (2021) 351–360, https://doi.org/10.1111/ijfs.15241.
[15] M. Kurdziel, K. Krolikowska, M. Labanowska, S. Pietrzyk, M. Michalec, The effect of thermal and irradiation treatments on structural and physicochemical properties

of octenyl succinate maize starches, Food Chem. 330 (2020), https://doi.org/10.1016/j.foodchem.2020.127242. Article 127242.
[16] L. Altuna, M.L. Herrera, M.L. Foresti, Synthesis and characterization of octenyl succinic anhydride modified starches for food applications. A review of recent literature, Food Hydrocoll. 80 (2018) 97–110, https://doi.org/10.1016/j.foodhyd.2018.01.032.
[17] N. Masina, Y.E. Choonara, P. Kumar, L.C. du Toit, M. Govender, S. Indermun, V. Pillay, A review of the chemical modification techniques of starch, Carbohydr. Polym. 157 (2017) 1226–1236, https://doi.org/10.1016/j.carbpol.2016.09.094.
[18] Q. Chen, H.J. Yu, L. Wang, Z. Ul Abdin, Y.S. Chen, J.H. Wang, W.D. Zhou, X. P. Yang, R.U. Khan, H.T. Zhang, X. Chen, Recent progress in chemical modification of starch and its applications, RSC Adv. 5 (2015) 67459–67474, https://doi.org/10.1039/C5RA10849G.
[19] M.M. Shi, Y. Jing, L.Z. Yang, X.Q. Huang, H.W. Wang, Y.Z. Yan, Y.Q. Liu, Structure and physicochemical properties of malate starches from corn, potato, and wrinkled pea starches, Polymers. 11 (2019), https://doi.org/10.3390/polym11091523. Article 1523.
[20] J.H. Chen, X. Chen, G.H. Zhou, X.L. Xu, New insights into the ultrasound impact on covalent reactions of myofibrillar protein, Ultrason. Sonochem. 84 (2022), https://doi.org/10.1016/j.ultsonch.2022.105973. Article 105973.
[21] S.J. Wang, J.R. Wang, S.K. Wang, S. Wang, Annealing improves paste viscosity and stability of starch, Food Hydrocoll. 62 (2017) 203–211, https://doi.org/10.1016/j.foodhyd.2016.08.006.
[22] M.M. Shi, X.W. Liang, Y.Z. Yan, H.H. Pan, Y.Q. Liu, Influence of ethanol-water solvent and ultra-high pressure on the stability of amylose-n-octanol complex, Food Hydrocoll. 74 (2018) 315–323, https://doi.org/10.1016/j.foodhyd.2017.08.003.
[23] Y.Q. Tian, Y. Li, X.M. Xu, Z.Y. Jin, Starch retrogradation studied by thermogravimetric analysis (TGA), Carbohydr. Polym. 84 (2011) 1165–1168, https://doi.org/10.1016/j.carbpol.2011.01.006.
[24] Y.Z. Yan, L.L. Feng, M.M. Shi, C. Cui, Y.Q. Liu, Effect of plasma-activated water on the structure and *in vitro* digestibility of waxy and normal maize starches during heat-moisture treatment, Food Chem. 306 (2020), https://doi.org/10.1016/j.foodchem.2019.125589. Article 125589.
[25] S.Y. Lee, K.Y. Lee, H.G. Lee, Effect of different pH conditions on the *in vitro* digestibility and physicochemical properties of citric acid-treated potato starch, Int. J. Biol. Macromol. 107 (2017) 1235–1241, https://doi.org/10.1016/j.ijbiomac.2017.09.106.
[26] H.N. Hao, Q. Li, W.J. Bao, Y.W. Wu, J. Ouyang, Relationship between physicochemical characteristics and *in vitro* digestibility of chestnut (*Castanea mollissima*) starch, Food Hydrocoll. 84 (2018) 193–199, https://doi.org/10.1016/j.foodhyd.2018.05.031.
[27] J.Y. Kim, Y.K. Lee, Y.H. Chang, Structure and digestibility properties of resistant rice starch cross-linked with citric acid, Int. J. Food Prop. 20 (2017) 2166–2177, https://doi.org/10.1080/10942912.2017.1368551.
[28] J.L. Shi, M.C. Sweedman, Y.C. Shi, Structural changes and digestibility of waxy maize starch debranched by different levels of pullulanase, Carbohydr. Polym. 194 (2018) 350–356, https://doi.org/10.1016/j.carbpol.2018.04.053.
[29] S. Garg, A.K. Jana, Characterization and evaluation of acylated starch with different acyl groups and degrees of substitution, Carbohydr. Polym. 83 (2011) 1623–1630, https://doi.org/10.1016/j.carbpol.2010.10.015.
[30] M. Miao, B. Jiang, T. Zhang, Effect of pullulanase debranching and recrystallization on structure and digestibility of waxy maize starch, Carbohydr. Polym. 76 (2009) 214–221, https://doi.org/10.1016/j.carbpol.2008.10.007.
[31] Y.Q. Liu, J.G. Liu, J. Kong, R. Wang, M. Liu, P. Strappe, C. Blanchard, Z.K. Zhou, Citrate esterification of debranched waxy maize starch: Structural, physicochemical and amylolysis properties, Food Hydrocoll. 104 (2020), https://doi.org/10.1016/j.foodhyd.2020.105704. Article 105704.
[32] K. Kaczmarska, B. Grabowska, A. Bobrowski, S. Cukrowicz, Effects of curing conditions on the structure of sodium carboxymethyl starch/mineral matrix system: FT-IR investigation, Spectrochimica Acta A Mol. Biomol. Spectrosc. 201 (2018) 236–241, https://doi.org/10.1016/j.saa.2018.04.049.
[33] S.Q. Tian, Y.Q. Yang, Molecular characteristics and digestion properties of corn starch esterified by L-malic acid, J. Food Process. Pres. 45 (2021), https://doi.org/10.1111/jfpp.15391. Article e15391.
[34] H. Abral, A. Basri, F. Muhammad, Y. Fernando, F. Hafizulhaq, M. Mahardika, E. Sugiarti, S.M. Sapuan, R.A. Ilyas, I. Stephane, A simple method for improving the properties of the sago starch films prepared by using ultrasonication treatment, Food Hydrocoll. 93 (2019) 276–283, https://doi.org/10.1016/j.foodhyd.2019.02.012.
[35] J.H. Chen, X. Zhang, X. Chen, A.P. Bassey, G.H. Zhou, X.L. Xu, Phenolic modification of myofibrillar protein enhanced by ultrasound: the structure of phenol matters, Food Chem. 386 (2022), https://doi.org/10.1016/j.foodchem.2022.132662. Article 132662.
[36] J.H. Na, G.A. Jeong, H.J. Park, C.J. Lee, Impact of esterification with malic acid on the structural characteristics and in vitro digestibilities of different starches, Int. J. Biol. Macromol. 174 (2021) 540–548, https://doi.org/10.1016/j.ijbiomac.2021.01.220.
[37] C. Ding, H.J. Zhang, S.Q. Zhao, Y. Luo, Q.H. Hu, Q. Liu, T. Tian, L.J. Zhang, X. R. Xue, Efficiency, functionality, and multi-scale structure of citric acid esterified glutinous rice starch synthesized via infrared radiation, Food Hydrocoll. 125 (2022), https://doi.org/10.1016/j.foodhyd.2021.107377. Article 107377.
[38] B. Gong, L.L. Cheng, R.G. Gilbert, C. Li, Distribution of short to medium amylose chains are major controllers of *in vitro* digestion of retrograded rice starch, Food Hydrocoll. 96 (2019) 634–643, https://doi.org/10.1016/j.foodhyd.2019.06.003.
[39] J.Q. Mei, D.N. Zhou, Z.Y. Jin, X.M. Xu, H.Q. Chen, Effects of citric acid esterification on digestibility, structural and physicochemical properties of cassava starch, Food Chem. 187 (2015) 378–384, https://doi.org/10.1016/j.foodchem.2015.04.076.
[40] B.Y. Chen, Z.B. Guo, S. Miao, S.X. Zeng, X.Z. Jia, Y. Zhang, B.D. Zheng, Preparation and characterization of lotus seed starch-fatty acid complexes formed by microfluidization, J. Food Eng. 237 (2018) 52–59, https://doi.org/10.1016/j.jfoodeng.2018.05.020.
[41] D.J. Jenkins, T.M. Wolever, R.H. Taylor, H. Barker, H. Fielden, J.M. Baldwin, A. C. Bowling, H.C. Newman, A.L. Jenkins, D.V. Goff, Glycemic index of foods: a physiological basis for carbohydrate exchange, Am. J. Clin. Nutr. 34 (1981) 362–366, https://doi.org/10.1093/ajcn/34.3.362.
[42] T.J. Gutiérrez, Characterization and *in vitro* digestibility of non-conventional starches from Guinea arrowroot and La Armuña lentils as potential food sources for special diet regimens, Starch-Stärke 70 (2018), https://doi.org/10.1002/star.201700124. Article 1700124.
[43] J.H. Chen, X. Chen, G.H. Zhou, X.L. Xu, Ultrasound: a reliable method for regulating food component interactions in protein-based food matrices, Trends Food Sci. Tech. 128 (2022) 316–330, https://doi.org/10.1016/j.tifs.2022.08.014.